

1           **A total energy error analysis of dynamical cores and**  
2           **physics-dynamics coupling in the Community Atmosphere**  
3           **Model (CAM)**

4           **Peter H. Lauritzen<sup>1\*</sup>, and David L. Williamson<sup>1</sup>**

5           <sup>1</sup>National Center for Atmospheric Research, Boulder, Colorado, USA

6           **Key Points:**

- 7           • Spurious total energy dissipation in dynamical core is  $-0.3W/m^2$  to  $-1W/m^2$  at 1  
8           degree  
9           • Constant-pressure assumption in physics leads to  $0.3W/m^2$  spurious total energy  
10          source  
11          • There can easily be compensating errors in total energy budget

---

\*1850 Table Mesa Drive, Boulder, Colorado, USA

Corresponding author: Peter Hjort Lauritzen, pel@ucar.edu

12 **Abstract**

13 A closed total energy (TE) budget is of utmost importance in coupled climate system  
 14 modeling; in particular, the dynamical core or physics-dynamics coupling should ideally  
 15 not lead to spurious TE sources/sinks. To assess this in a global climate model, a detailed  
 16 analysis of the spurious sources/sinks of TE in NCAR's Community Atmosphere Model  
 17 (CAM) is given. This includes spurious sources/sinks associated with the parameteriza-  
 18 tion suite, the dynamical core, TE definition discrepancies and physics-dynamics coupling.  
 19 The latter leads to a detailed discussion of the pros and cons of various physics-dynamics  
 20 coupling methods commonly used in climate/weather modeling.

21 **1 Introduction**

22 In coupled climate modeling with prognostic atmosphere, ocean, land, land-ice, and  
 23 sea-ice components, it is important to conserve total energy (TE) to a high degree in each  
 24 component individually and in the complete model to avoid spurious long term trends in  
 25 the simulated Earth system. Conservation of TE in this context refers to having a closed  
 26 TE budget. For example, the TE change in a column in the atmosphere is exactly balanced  
 27 by the net sources/sinks given by the fluxes through the column. The fluxes into the at-  
 28 mospheric component from the surface models must be balanced by the fluxes in the re-  
 29 spective surface components and so on. Henceforth we will focus only on the atmospheric  
 30 component which, in a numerical model, is split into a resolved-scale component (the dy-  
 31 namical core) and a sub-grid-scale component (parameterizations or, in modeling jargon,  
 32 physics). While there have been many studies on energy flow in the Earth system through  
 33 analysis of re-analysis data and observations [Trenberth and Fasullo, 2018, and references  
 34 herein], there has been less focus on spurious TE sources/sinks in numerical models.

35 The atmospheric equations of motion conserve TE but the discretizations used in cli-  
 36 mate and weather models are usually not inherently TE conservative. Exact conservation  
 37 is probably not necessary but conservation to within  $\sim 0.01 \text{ W/m}^2$  has been considered  
 38 sufficient to avoid spurious trends in century long simulations [Boville, 2000; Williamson  
 39 *et al.*, 2015]. Spurious sources and sinks of TE can be introduced by the dynamical core,  
 40 physics, physics-dynamics coupling as well as discrepancies between the TE of the con-  
 41 tinuous and discrete equations of motion and for the physics. Hence the study of TE con-  
 42 servation in comprehensive models of the atmosphere quickly becomes a quite complex  
 43 and detailed matter. In addition there can easily be compensating errors in the system as a  
 44 whole.

45 Here we focus on versions of the Community Atmosphere Model (CAM) that use  
 46 the spectral-element [SE, Lauritzen *et al.*, 2018] and finite-volume [FV, Lin, 2004] dy-  
 47 namical cores. These dynamical cores couple with physics in a time-split manner, i.e.  
 48 physics receives a state updated by dynamics [see Williamson, 2002, for a discussion  
 49 of time-split versus process split physics-dynamics coupling in the context of CAM]. In  
 50 its pure time-split form the physics tendencies are added to the state previously produced  
 51 by the dynamical core and the resulting state provides the initial state for the subsequent  
 52 dynamical core calculation. We refer to this as *state-updating* (`ftype=1` in CAM code).  
 53 Alternatively, when the dynamical core adopts a shorter time step than the physics, say  
 54 `nsplit` sub-steps, then  $(1/\text{nsplit})$ th of the physics-calculated tendency is added to the  
 55 state before each dynamics sub-step. We refer to this modification of time-splitting as  
 56 *dribbling* (`ftype=0`). CAM-FV uses the *state-update* (`ftype=1`) approach while CAM-SE  
 57 has options to use *state-update* (`ftype=1`), *dribbling* (`ftype=0`) or a combination of the  
 58 two i.e. mass-variables use *state-updating* and remaining variables use *dribbling*. We refer  
 59 to this as *combination* (`ftype=2`). The *dribbling* variants can lead to spurious sources or  
 60 sinks of TE (and mass) referred to here as physics-dynamics coupling errors.

61 The dynamical core usually has inherent or specified filters to control spurious noise  
 62 near the grid scale which will lead to energy dissipation [Thuburn, 2008; Jablonowski

and Williamson, 2011]. Similarly models often have sponge layers to control the solution near the top of the model that may be a sink of TE. There are examples of numerical discretizations of the adiabatic frictionless equations motion that are designed so that TE is conserved in the absence of time-truncation and filtering errors [e.g., Eldred and Randall, 2017; McRae and Cotter, 2013], e.g., mimetic spectral-element discretizations such as the one used in the horizontal in CAM-SE [Taylor, 2011]. These provide consistency between the discrete momentum and thermodynamic equations leading to global conservation associated with the conversion of potential to kinetic energy. In spectral transform models it is customary to add the energy change due to explicit diffusion on momentum back as heating (referred to as frictional heating), so that the diffusion of momentum does not affect the TE budget [see, e.g., p.71 in Neale et al., 2012]. This is also done in CAM-SE [Lauritzen et al., 2018].

The purpose of this paper is to provide a detailed global TE analysis of CAM. We assess TE errors due to various steps in the model algorithms. The paper is outlined as follows. In section 2 the continuous TE formulas are given and a detailed description of spurious TE sources/sinks that can occur in a model as a whole, and the associated diagnostics used to perform the TE analysis, are defined. In section 3 the model is run in various configurations to assess their effects on TE conservation. This includes various physics-dynamics coupling experiments leading to a rather detailed discussion of mass budget closure. We also investigate the effect of using a limiter in the vertical remapping of momentum, assess energy discrepancy errors and impacts on TE of simplifying surface conditions and dry atmosphere experiments. The paper ends with conclusions.

## 2 Method

### 2.1 Defining total energy (TE)

In the following it is assumed that the model top and bottom are coordinate surfaces and that there is no flux of mass through the model top and bottom. In a dry hydrostatic atmosphere the TE equation integrated over the entire sphere is given by

$$\frac{d}{dt} \int_{z=z_s}^{z=z_{top}} \iint_S E_v \rho^{(d)} dA dz = \int_{z=z_s}^{z=z_{top}} \iint_S F_{net} \rho^{(d)} dA dz, \quad (1)$$

[e.g., Kasahara, 1974] where  $F_{net}$  is net flux calculated by the parameterizations (e.g., heating and momentum forcing),  $d/dt$  the total/material derivative,  $z_s$  is the height of the surface,  $S$  the sphere,  $\rho^{(d)}$  the density of dry air,  $E_v$  is the TE and  $dA$  is an infinitesimal area on the sphere.  $E_v$  can be split into kinetic energy  $K = \frac{1}{2}\mathbf{v}^2$  ( $\mathbf{v}$  is the wind vector), internal energy  $c_v^{(d)}T$ , where  $c_v^{(d)}$  is the heat capacity of dry air at constant volume, and potential energy  $\Phi = gz$

$$E_v = K + c_v^{(d)}T + \Phi. \quad (2)$$

If the vertical integral is performed in a mass-based vertical coordinate, e.g., pressure, then the integrated TE equation for a dry atmosphere can be written as

$$\frac{d}{dt} \int_{p=p_s}^{p=p_{top}} \iint_S E_p dA dp + \frac{d}{dt} \iint_S \Phi_s p_s dA = \int_{p=p_s}^{p=p_{top}} \iint_S F_{net} dA dp, \quad (3)$$

[e.g., Kasahara, 1974] where

$$E_p = K + c_p^{(d)}T. \quad (4)$$

In a moist atmosphere, however, there are several definitions of TE used in the literature related to what heat capacity is used for water vapor and whether or not condensates are accounted for in the energy equation. To explain the details of that we focus on the energy equation for CAM-SE.

CAM-SE is formulated using a terrain-following hybrid-sigma vertical coordinate  $\eta$  but the coordinate levels are defined in terms of dry air mass per unit area ( $M^{(d)}$ ) instead of total air mass;  $\eta^{(d)}$  [see Lauritzen et al., 2018, for details]. In such a coordinate

106 system it is convenient to define the tracer state in terms of a dry mixing ratio instead of  
 107 moist mixing ratio

$$m^{(\ell)} \equiv \frac{\rho^{(\ell)}}{\rho^{(d)}}, \text{ where } \ell = 'wv', 'cl', 'ci', 'rn', 'sw', \quad (5)$$

108 where  $\rho^{(d)}$  is the mass of dry air per unit volume of moist air and  $\rho^{(\ell)}$  is the mass of the  
 109 water substance of type  $\ell$  per unit volume of moist air. Moist air refers to air containing  
 110 dry air ('d'), water vapor ('wv'), cloud liquid ('cl'), cloud ice ('ci'), rain amount ('rn')  
 111 and snow amount ('sw'). For notational purposes define the set of all components of air

$$\mathcal{L}_{all} = \{'d', 'wv', 'cl', 'ci', 'rn', 'sw'\}, \quad (6)$$

112 Define associated heat capacities at constant pressure  $c_p^{(\ell)}$ . We refer to condensates as being  
 113 *thermodynamically and inertially active* if they are included in the thermodynamic  
 114 equation and momentum equations. E.g. if the thermodynamic equation is formulated  
 115 in terms of temperature the energy conversion term includes a generalized heat capacity  
 116 which is a function of the condensates and their associated heat capacities [see, e.g., sec-  
 117 tion 2.3 in *Lauritzen et al., 2018*]. Similarly the weight of the condensates is included in  
 118 the pressure field and pressure gradient force. How many and which condensates are ther-  
 119 modynamically/inertially active in the dynamical core is controlled with namelist `qsize_condensate_loading`.  
 120 If `qsize_condensate_loading=1` only water vapor ('wv') is active, `qsize_condensate_loading=3`  
 121 'wv', 'cl', and 'ci' are active, and if `qsize_condensate_loading=5` then 'wv', 'cl', 'ci', 'rn',  
 122 and 'sw' are included.

123 Using the  $\eta^{(d)}$  vertical coordinate and dry mixing ratios the TE (per unit area) that  
 124 the frictionless adiabatic equations of motion in the CAM-SE dynamical core conserves is

$$\widehat{E}_{dyn} = \frac{1}{\Delta S} \int_{\eta=0}^{\eta=1} \iint_S \left( \frac{1}{g} \frac{\partial M^{(d)}}{\partial \eta^{(d)}} \right) \sum_{\ell \in \mathcal{L}_{all}} \left[ m^{(\ell)} (K + c_p^{(\ell)} T + \Phi_s) \right] dA d\eta^{(d)}, \quad (7)$$

125 where  $\Delta S$  is the surface area of the sphere,  $\Phi_s$  is the surface geopotential and  $(\cdot)$  refers to  
 126 the global average.

127 In the CAM physical parameterizations a different definition of TE is used. Due to  
 128 the evolutionary nature of the model development, the parameterizations have not yet been  
 129 converted to match the SE dynamical core. For the computation of TE, condensates are  
 130 assumed to be zero and the heat capacity of moisture is the same as for dry air. This is  
 131 equivalent to using a moist mass (dry air plus water vapor) but  $c_p$  of dry air:

$$\widehat{E}_{phys} = \frac{1}{\Delta S} \int_{\eta=0}^{\eta=1} \iint_S \left( \frac{1}{g} \frac{\partial M^{(d)}}{\partial \eta^{(d)}} \right) \left( 1 + m^{(wv)} \right) \left[ (K + c_p^{(d)} T + \Phi_s) \right] dA d\eta^{(d)}. \quad (8)$$

132 We note that earlier versions of CAM using the spectral transform dynamical core used  
 133  $c_p$  of moist air. The adiabatic, frictionless equations of motion in the CAM-SE dynamical  
 134 core can be made consistent with  $E_{phys}$  by not including condensates in the mass/pressure  
 135 field as well as energy conversion term in the thermodynamic equation and setting the  
 136 heat capacity for moisture to  $c_p^{(d)}$  [Taylor, 2011]. We refer to this version of CAM-SE as  
 137 the *energy consistent* version.

## 138 2.2 Some remarks on local total energy conservation

139 [I think you missed an opportunity to remind the reader of the additional complex-  
 140 ities of a moist atmosphere here. The development and discussion is currently entirely  
 141 framed in term of the global integrals, but maybe you should say that there are local con-  
 142 siderations at play also. Whenever an air parcel containing water undergoes a phase change  
 143 its temperature should change, and its energy (enthalpy), and mass should not. When the  
 144 air parcel gains or loses water via sedimentation or precipitation or via a fixer or borrower  
 145 to maintain some physical property like positive definiteness, then it has implications for

146 the mass and heat content of the parcel, and the heat capacity of the parcel. And that  
 147 affects the energy and mass of the column, and that affects the global energy. So any-  
 148 thing that changes these state variables locally has implications for the energy budget. I  
 149 think you need these kind of statements to be able to say that the current model frame-  
 150 work only tries to account for some of the terms in the energy and mass budget, and also  
 151 treats only a subset of the heat capacities/latent heat of fusion and vaporization. So when  
 152 surface pressure is fixed during a physical parameterization update but the water vapor is  
 153 changed an inconsistency appears. If a clipper is used on vapor or condense water, that is  
 154 a spurious source of water, but it is not accounted for in the thermodynamics, or through a  
 155 surface flux. Etc. I think it is worth saying this kind of stuff before you get into the global  
 156 integrals because it won't necessarily be obvious to the audience how for the example of  
 157 figure 5, that clipping of cloud water will produce an energy source or sink. ]

### 158 2.3 Spurious energy sources and sinks

159 In a weather/climate model TE conservation errors can appear in many places through-  
 160 out the algorithm. Below is a general list of where conservation errors can appear with  
 161 specific examples from CAM:

- 162 1. *Parameterization errors*: Individual parameterizations may not have a closed en-  
 163 ergy budget. CAM parameterizations are required to have a closed energy budget  
 164 under the assumption that pressure remains constant during the computation of the  
 165 subgrid-scale parameterization tendencies. In other words, the TE change in the  
 166 column is exactly balanced by the net sources/sinks given by the fluxes through the  
 167 column.
- 168 2. *Pressure work error*: That said, if parameterizations update specific humidity then  
 169 the surface pressure changes (e.g., moisture entering or leaving the column). In  
 170 that case the pressure changes which, in turn, changes TE. This is referred to as  
 171 *pressure work error* [section 3.1.8 in *Neale et al., 2012*].
- 172 3. *Continuous TE formula discrepancy*: If the continuous equations of motion for the  
 173 dynamical core conserve a TE different from the one used in the parameterizations  
 174 then an energy inconsistency is present in the system as a whole. This is the case  
 175 with the new version of CAM-SE that conserves a TE that is more accurate and  
 176 comprehensive than that used in the CAM physics package as discussed above. As  
 177 also noted above, this mismatch arose from the evolutionary nature of the model  
 178 development and not by deliberate design; and should be eliminated in the future.
- 179 4. *Dynamical core errors*: [mention that we assume that dynamical core is inherently  
 180 mass conservative] Energy conservation errors in the dynamical core, not related to  
 181 physics-dynamics coupling errors, can arise in multiple parts of the algorithms used  
 182 to solve the equations of motion. For dynamical cores employing filtering [e.g.,  
 183 limiters in flux operators *Lin, 2004*] and/or possessing inherent damping which  
 184 controls small scales, it is hard to isolate their energy dissipation from other errors  
 185 in the discretization. If a hyperviscosity term or some other diffusion is added to  
 186 the momentum equation, then one can diagnose the local energy dissipation from  
 187 such damping and add a corresponding heating to balance it (frictional heating).  
 188 There may also be energy loss from viscosity applied to other variables such a tem-  
 189 perature or pressure which is harder to compensate. Here is a break-down relevant  
 190 to CAM-SE using a floating Lagrangian vertical coordinate:
  - 191 • Horizontal inviscid dynamics: Energy errors resulting from solving the inviscid,  
 192 adiabatic equations of motion.
  - 193 • Hyperviscosity: Filtering errors.
  - 194 • Vertical remapping: The vertical remapping algorithm from Lagrangian to Eule-  
 195 rian reference surfaces does not conserve TE.

- 196 • Near round-off negative values of water vapor which are filled to a minimal  
 197 value without compensation.

198 If a dynamical core is not inherently mass-conservative with respect to dry air, wa-  
 199 ter vapor and condensates then TE conservation is affected since

$$\int_{\eta=0}^{\eta=1} \iint_S \left( \frac{1}{g} \frac{\partial M^{(d)}}{\partial \eta^{(d)}} \right) \sum_{\ell \in \mathcal{L}_{all}} [m^{(\ell)}] dA d\eta^{(d)} \quad (9)$$

200 is not conserved. Henceforth we assume that the dynamical core is based on an  
 201 inherently mass-conservative formulation which is the case for CAM-SE and CAM-  
 202 FV.

203 5. *Physics-dynamics coupling (PDC)*: Assume that physics computes a tendency. Usu-  
 204 ally the tendency (forcing) is passed to the dynamical core which is responsible for  
 205 adding the tendencies to the state. PDC energy errors can be split into three types:

- 206 • ‘Dribbling’ errors (or, equivalently, temporal PDC errors): If the TE increment  
 207 from the parameterizations does not match the change in TE when the tenden-  
 208 cies are added to the state in the dynamical core, then there will be a spurious  
 209 PDC error. This will not happen with the *state-update* approach in which the  
 210 tendencies are added immediately after physics and before the dynamical core  
 211 advances the solution in time. The PDC ‘dribblin’ errors can be split into 3 con-  
 212 tributions:.

213 *Thermal energy ‘dribbling’ error*: PDC errors in temperature tendencies occur  
 214 because the  $T$ -increment (call it  $\Delta T$ ) that the parameterizations prescribe leads  
 215 to a dry thermal energy change of  $\Delta M^{(d)} \Delta T$  which will not match the equivalent  
 216 dry thermal energy change when the temperature tendency is added in smaller  
 217 chunks in the dynamical core during the ‘dribbling’ of  $\Delta T$ . The discrepancy  
 218 occurs because  $\Delta M^{(d)}$  changes during each dynamics time-step and hence the  
 219 thermal energy change due to physics forcing accumulated during the ‘dribbling’  
 220 will not equal  $\Delta M^{(d)} \Delta T$ . This error could possibly be eliminated by using ther-  
 221 mal energy forcing instead of temperature increments.

222 *Kinetic energy ‘dribbling’ error*: Similarly, PDC errors in velocity component  
 223 forcing increments ( $\Delta u, \Delta v$ ) occur because the dry kinetic energy change of  $\Delta M^{(d)} [(\Delta u)^2 + (\Delta v)^2]$   
 224 will not match the equivalent dry kinetic energy change when ‘dribbling’ veloc-  
 225 ity component forcing increments ( $\Delta u, \Delta v$ ). It is less clear how to eliminate this  
 226 error as kinetic energy is a quadratic quantity.

227 *Mass ‘clipping’ (affects all TE terms)*: A similar PDC error for mass-variables  
 228 such as vapor vapor forcing, cloud liquid, etc. can occur when the mass-tendencies  
 229 are ‘dribbled’ during the dynamical core integration. The dynamical core trans-  
 230 port of mass variables will move mass around in the horizontal and vertical while  
 231 the ‘dribbled’ physics mass increments are applied in the same location, the  
 232 mass-increment from the parameterizations may be larger than the mass avail-  
 233 able. This can lead to a spurious source mass if there is logic in the dynamical  
 234 core preventing mixing ratios/mass to become negative. This is referred to as  
 235 ‘clipping’ PDC errors and precess is described/discussed in detail in Section  
 236 3.2.1. The ‘clipping’ change the water mass budget without accounting for it in  
 237 water fluxes or in the thermodynamics and hence lead to a TE conservation er-  
 238 rors (both kinetic and thermal energy).

- 239 • *Change of vertical grid/coordinate errors*: If the vertical coordinates in physics  
 240 and in the dynamical core are different then there can be spurious PDC energy  
 241 errors even when using the state-update method for adding tendencies to the dy-  
 242 namical core state. For example, many non-hydrostatic dynamical cores [e.g.  
 243 Skamarock et al., 2012] use a terrain-following height coordinate whereas physics  
 244 uses pressure.
- 245 • *Change of horizontal grid errors*: If the physics tendencies are computed on a  
 246 different horizontal grid than the dynamical core then there can be spurious en-

247        ergy errors from mapping tendencies and/or variables between horizontal grids  
 248        [e.g., *Herrington et al.*, 2018].

- 249        6. *Compensating Energy fixers:* To avoid TE conservation errors which could accu-  
 250        mulate and ultimately lead to a climate drift, it is customary to apply an arbitrary  
 251        energy fixer to restore TE conservation. Since the spatial distribution of many en-  
 252        ergy errors, in general, is not known, global fixers are used. In CAM a uniform in-  
 253        crement is added to the temperature field to compensate for TE imbalance from all  
 254        processes, i.e. dynamical core, physics-dynamics coupling, TE formula discrepancy,  
 255        energy change due to pressure work **error**, and possibly parameterization errors if  
 256        present.

257        **2.4 Diagnostics**

258        The discrete global averages  $(\hat{\cdot})$  are computed consistent with the discrete model grid  
 259        as outlined in section 2.2. of *Lauritzen et al.* [2014]. The TE global average tendency is  
 260        denoted

$$\partial \hat{E} \equiv \frac{d\hat{E}}{dt}. \quad (10)$$

261        By computing the global TE averages  $\hat{E}$  at appropriate places in the model algorithms,  
 262        we can directly compute  $\partial \hat{E}$  due to various processes (such as viscosity, vertical remap-  
 263        ping, physics-dynamics coupling, pressure work **error**, etc.) by differencing  $\hat{E}$  from after  
 264        and before the algorithm takes place. This has been implemented using CAM history in-  
 265        frastructure by computing column integrals of energy at various places in CAM and out-  
 266        putting the 2D energy fields. CAM history internally handles accumulation and averag-  
 267        ing in time at each horizontal grid point. The global averages are computed externally  
 268        from the grid point vertical integrals on the history files (stored in double precision). The  
 269        places in CAM where we compute/capture the grid point vertical integral  $E$  are named us-  
 270        ing three letters where the first letter refers to whether the vertical integral is performed  
 271        in physics ('p') or in the dynamical core ('d'). The trailing two letters refer to the specific  
 272        location in dynamics or physics. For example, 'BP' refers to 'Before Physics' and 'AP'  
 273        to 'After Physics'; the associated total energies are denoted  $E_{pBP}$  and  $E_{pAP}$ , respectively.  
 274        The TE tendency from the parameterizations is the difference between  $E_{pBP}$  and  $E_{pAP}$   
 275        divided by the time-step. The terms and tendencies are then averaged globally externally  
 276        to the model. The pseudo-code in Figure 1 defines the acronyms in terms of where in the  
 277        CAM-SE algorithm the TE vertical integrals are computed and output. For details on the  
 278        CAM-SE algorithm please see *Lauritzen et al.* [2018].

279        Before defining the individual terms in detail we briefly review the model time step-  
 280        ping sequence starting with the physics component as illustrated in Figure 1. The energy  
 281        fixer is applied first to compensate for the spurious net energy change from all compo-  
 282        nents introduced during the previous time step. We will describe this in more detail af-  
 283        ter the various sources and sinks are elucidated. The parameterizations are applied next  
 284        and are required to be energy conserving. They update the state and accumulate the total  
 285        physics tendency (forcing). At this stage the state is saved for use in the energy fixer in  
 286        the next time step. Any changes in the global average energy after this are spurious and  
 287        are compensated by the fixer. The parameterizations update the water vapor but not the  
 288        moist pressure, implying a non-physical change in the dry mass of the atmosphere. The  
 289        dry mass correction corrects the dry mass back to its proper value.

290        The forcing (physics tendency) from the parameterizations is passed to the dynam-  
 291        ical core. If the physics and dynamics operate on different grids, the forcing is remapped  
 292        here. The dynamics operates on a shorter time step **than** the physics and is sub-stepped.  
 293        The remapped **physics increment** is applied to the dynamics state, saved from the end of  
 294        the previous dynamics step, using either *state-updating*, *dribbling*, or *combination* as de-  
 295        scribed in the introduction. The dynamics then advances the adiabatic frictionless flow in  
 296        the floating Lagrangian layers over a further set of sub-steps. Hyperviscosity is applied

next with further sub-stepping required for computational stability of the explicit discrete approximations. The energy loss from the specified momentum viscosity is calculate locally and is balanced by adding a local change to the temperature, referred to as *frictional heating*. This set of dynamics sub-steps is followed by the vertical remapping from Lagrangian to Eulerian reference layers. The remapping is required to provide layers consistent with the parameterization formulations. The vertical remapping sub-steps are required for stability if the Lagrangian layers become too thin.

At the end of the dynamics, the state is saved to be used by the dynamics the next time step and is also passed to the physics, with a remapping if the dynamics and physics grids differ. At the beginning of the physics the difference in energy between this state and the state saved after the physics during the previous time step is the amount needed to be added or subtracted by the energy fixer. It represents the accumulation of all spurious sources from the dry mass correction, remappings between physics and dynamics grids (if applicable), dynamical core, differing energy definitions (if present), hyerviscosity, and vertical remapping.

We now define the following energy tendencies corresponding to the itemized list in section 2.2 with references to terms indicated in Figure 1. We start just after the energy fixer which will be defined at the end.

1.  $\partial \widehat{E}^{(param)}$ : TE tendency due to parameterizations. In CAM the TE budget for each parameterization is closed (assuming pressure is unchanged) so  $\partial \widehat{E}^{(param)}$  is balanced by net fluxes in/out of the physics columns. Note that this is the only energy tendency that is not spurious since CAM parameterizations have a closed TE budget. This TE tendency is discretely computed as

$$\partial \widehat{E}_{phys}^{(param)} = \frac{\widehat{E}_{pAP} - \widehat{E}_{pBP}}{\Delta t_{phys}}, \quad (11)$$

where  $\Delta t_{phys}$  is the physics time-step (default 1800s) and the subscript *phys* on  $\partial \widehat{E}$  refers to the energy tendency computed in CAM physics.

2.  $\partial \widehat{E}^{(pwork)}$ : Total spurious energy tendency due to pressure work **error**

$$\partial \widehat{E}_{phys}^{(pwork)} = \frac{\widehat{E}_{pAM} - \widehat{E}_{pAP}}{\Delta t_{phys}}. \quad (12)$$

Since CAM-SE dynamical core is based on a dry-mass vertical coordinate the pressure work **error** takes place implicitly in the dynamical core. But the TE tendency due to pressure work **error** is conveniently computed in physics since dynamical cores based on a moist vertical coordinate (e.g., CAM-FV) require pressure and moist mixing ratios to be adjusted for dry mass conservation and tracer mass conservation [section 3.1.8 in *Neale et al.*, 2012]. The difference of TE after and before this adjustment is the TE tendency due to pressure work **error**. In a dry mass vertical coordinate based on dry mixing ratios neither dry mass layer thickness nor dry mixing ratios need to be adjusted to take into account moisture changes in the column. For labeling purposes, the 'total forcing' associated with physics (at least in CAM) consists of parameterizations, pressure work **error** and TE fixer, although strictly speaking the fixer includes components from the dynamics as will be seen.

$$\partial \widehat{E}_{phys}^{(phys)} \equiv \partial \widehat{E}_{phys}^{(param)} + \partial \widehat{E}_{phys}^{(pwork)} + \partial \widehat{E}_{phys}^{(efix)} = \frac{\widehat{E}_{pAM} - \widehat{E}_{pBF}}{\Delta t_{phys}}. \quad (13)$$

where the energy fixer TE tendency is

$$\partial \widehat{E}_{phys}^{(efix)} = \frac{\widehat{E}_{pBP} - \widehat{E}_{pBF}}{\Delta t_{phys}}. \quad (14)$$

- 344 After all the TE budget terms have been defined, the exact composition of  $\partial\widehat{E}_{phys}^{(efix)}$   
 345 will be presented.
- 346 3.  $\partial\widehat{E}^{(discr)}$ : If the physics uses a TE definition different from the TE that the  
 347 continuous equations of motion in the dynamical core conserve (i.e. in the absence of  
 348 discretization errors), then there is a TE discrepancy tendency. This complicates  
 349 the energy analysis as one can not compare TE computed in physics  $\widehat{E}_{phys}$  directly  
 350 with TE computed in the dynamical core  $\widehat{E}_{dyn}$ . This makes errors associated with  
 351 this discrepancy tricky to assess. That said, the TE tendencies computed using the  
 352 dynamical core TE formula  $\partial\widehat{E}_{dyn}$  are well defined (self consistent) and similarly  
 353 for TE tendencies computed using the ‘physics formula’ for TE,  $\partial\widehat{E}_{phys}$ .
- 354 4. The TE tendency from the dynamical core is split into several terms: Horizontal  
 355 adiabatic dynamics (dynamics excluding physics forcing tendency)

$$\partial\widehat{E}_{dyn}^{(2D)} = \frac{\widehat{E}_{dAD} - \widehat{E}_{dBD}}{\Delta t_{dyn}}, \quad (15)$$

356 where over a single dynamics sub-step  $\Delta t_{dyn} = \frac{\Delta t_{phys}}{n_{split} \times r_{split}}$  (the loop bounds  
 357  $n_{split}$ ,  $r_{split}$ , etc. are explained in Figure 1).

358 In CAM-SE the viscosity is explicit so one can compute the TE tendency due to  
 359 hyperviscosity and its associated frictional heating

$$\partial\widehat{E}_{dyn}^{(hvvis)} = \frac{\widehat{E}_{dAH} - \widehat{E}_{dBH}}{\Delta t_{hvvis}}, \quad (16)$$

360 which, in CAM-SE, includes a frictional heating term from viscosity on momentum

$$\partial\widehat{E}_{dyn}^{(fheat)} = \frac{\widehat{E}_{dAH} - \widehat{E}_{dCH}}{\Delta t_{hvvis}}, \quad (17)$$

361 where  $\Delta t_{hvvis} = \frac{\Delta t_{phys}}{n_{split} \times r_{split} \times hypervis\_subcycle}$  is the time step of the sub-stepped  
 362 viscosity. The residual

$$\partial\widehat{E}_{dyn}^{(res)} = \partial\widehat{E}_{dyn}^{(2D)} - \partial\widehat{E}_{dyn}^{(hvvis)}, \quad (18)$$

363 is the energy error due to inviscid dynamics and time-truncation errors.

364 The energy tendency due to vertical remapping is

$$\partial\widehat{E}_{dyn}^{(remap)} = \frac{\widehat{E}_{dAR} - \widehat{E}_{dAD}}{\Delta t_{remap}}, \quad (19)$$

365 where  $\Delta t_{remap} = \frac{\Delta t_{phys}}{n_{split}}$ .

366 The 3D adiabatic dynamical core (no physics forcing but including friction) energy  
 367 tendency is denoted

$$\partial\widehat{E}_{dyn}^{(adiab)} = \partial\widehat{E}_{dyn}^{(2D)} + \partial\widehat{E}_{dyn}^{(remap)}. \quad (20)$$

- 368 5.  $\partial\widehat{E}^{(pdc)}$ : Total spurious energy tendency due to physics-dynamics coupling errors is  
 369 the difference between the energy tendency from physics and the energy tendency  
 370 in the dynamics resulting from adding the physics increment to the dynamical core  
 371 state

$$\partial\widehat{E}^{(pdc)} = \partial\widehat{E}_{phys}^{(phys)} - \partial\widehat{E}_{dyn}^{(phys)} \text{ assuming } \partial\widehat{E}^{(discr)} = 0, \quad (21)$$

372 where

$$\partial\widehat{E}_{dyn}^{(phys)} = \frac{\widehat{E}_{dBD} - \widehat{E}_{dAF}}{\Delta t_{pdc}}, \quad (22)$$

373 and  $\Delta t_{pdc}$  is the time-step between physics increments being added to the dynami-  
 374 cal core. Remember we are dealing with average rates so terms computed with dif-  
 375 ferent time steps can be compared, but differences cannot be taken between terms  
 376 sampled with different time steps.

The physics-dynamics coupling TE tendency  $\partial\widehat{E}^{(pdc)}$  makes use of TE formulas in dynamics and in physics so (20) is only well-defined if the TE formula discrepancy is zero,  $\partial\widehat{E}^{(discr)} = 0$ . As mentioned in Section 2.1, CAM-SE has the option to switch the continuous equations of motion conserving the TE used by CAM physics (8) instead of the more comprehensive TE formula (7).

In CAM-SE there are 3 physics-dynamics coupling algorithms described in detail in section 3.6 in *Lauritzen et al. [2018]* and reviewed in the introduction here. One is *state-update* in which the entire physics increments are added to the dynamics state at the beginning of dynamics (referred to as `ftype=1`), in which case  $\Delta t_{pdc} = \Delta t_{phys}$ . Another is *dribbling* in which the physics tendency is split into `nsplit` equal chunks and added throughout dynamics (more precisely after every vertical remapping; referred to as `ftype=0` resulting in  $\Delta t_{pdc} = \frac{1}{nspit}\Delta t_{phys}$ ), and then a *combination* of the two (referred to as `ftype=2`) where tracers (mass variables) use *state-update* (`ftype=1`) and all other physics tendencies use *dribbling* (`ftype=0`).

6.  $\partial\widehat{E}^{(efix)}$ : Global energy fixer tendency, defined in (13), is applied at the beginning of the parameterizations. The correction needed is the global average difference between the state passed from the dynamics and the state that was saved after the physics updated the state but before the dry mass correction. It includes all spurious sources from the dry mass correction, remappings between physics and dynamics, dynamical core, differing energy definitions (if present), hyperviscosity, and vertical remapping.

## 2.5 A few observations regarding the energy budget terms

It is useful to note that the energy fixer ‘fixes’ energy errors for the dynamical core, pressure work **error**, physics-dynamics coupling and TE discrepancy

$$-\partial\widehat{E}_{phys}^{(efix)} = \partial\widehat{E}_{phys}^{(pwork)} + \partial\widehat{E}_{dyn}^{(adiab)} + \partial\widehat{E}^{(pdc)} + \partial\widehat{E}^{(discr)}. \quad (23)$$

The forcing from the parameterizations,  $\partial\widehat{E}_{phys}^{(param)}$ , does not appear in this budget (although the dynamical core state does ‘feel’ the parameterization forcing) as the energy cycle for the parameterizations is, by design in CAM, closed (balanced by fluxes in/out of the physics columns). If  $\partial\widehat{E}^{(discr)} = 0$ , one can use (22) to diagnose energy dissipation in the dynamical core and physics-dynamics coupling from quantities computed only in physics

$$\partial\widehat{E}_{dyn}^{(adiab)} + \partial\widehat{E}^{(pdc)} = -\partial\widehat{E}_{phys}^{(efix)} - \partial\widehat{E}_{phys}^{(pwork)} \text{ for } \partial\widehat{E}^{(discr)} = 0. \quad (24)$$

This is useful if the diagnostics are not implemented in the dynamical core; in particular, if the *state-update* (`ftype=1`) physics-dynamics coupling method is used then  $\partial\widehat{E}^{(pdc)} = 0$  and the TE errors in the dynamical core can be computed without diagnostics implemented in the dynamical core. Also, (23) provides an alternative formula for  $\partial\widehat{E}^{(pdc)}$  compared to (20):

$$\partial\widehat{E}^{(pdc)} = -\partial\widehat{E}_{phys}^{(efix)} - \partial\widehat{E}_{phys}^{(pwork)} - \partial\widehat{E}_{dyn}^{(adiab)} \text{ assuming } \partial\widehat{E}^{(discr)} = 0. \quad (25)$$

If  $\partial\widehat{E}^{(pdc)} = 0$  (22) can be used to compute  $\partial\widehat{E}^{(discr)}$

$$\partial\widehat{E}^{(discr)} = -\partial\widehat{E}_{phys}^{(efix)} - \partial\widehat{E}_{phys}^{(pwork)} - \partial\widehat{E}_{dyn}^{(adiab)}, \text{ assuming } \partial\widehat{E}^{(pdc)} = 0. \quad (26)$$

Note that we can not use (20) to compute  $\partial\widehat{E}^{(discr)}$  since  $\widehat{E}_{phys} \neq \widehat{E}_{dyn}$ .

## 3 Results

A series of simulations have been performed with CESM2.1 using CAM version 6 (CAM6) physics (<https://doi.org/10.5065/D67H1H0V>) on NCAR’s Cheyenne cluster [*Computational and Information Systems Laboratory, 2017*]. All simulations are at nominally  $\sim 1^\circ$  horizontal resolution (for CAM-SE that is 30×30 elements on each cubed-sphere face and for CAM-FV its 192×288 latitudes-longitudes) and using the standard

**Table 1.** TE tendencies in units of  $W/m^2$  associated with various aspects of CAM-SE run in AMIP-type setup (unless otherwise noted). Column 1 is the identifier for the model configuration. See the text for a brief summary of these descriptors. They are defined in more detail in the following sections where the section titles also include the ‘Descriptor’ from Table 1 to make it easier for the reader to match Table entries with discussion in the text. Column 2 is  $N = \text{qsize\_condensate\_loading}$  identifying how many water species are thermodynamically/**inertially** active in the dynamical core (see section 2.1 for details). Column 3,  $\text{lcp\_moist}$ , indicates whether or not the heat capacity includes water variables or not and column 4 shows physics-dynamics coupling method  $f_{\text{type}}$ . The TE tendencies  $\partial \hat{E}$  in columns 5-14 are defined in section 2.3. If  $\partial \hat{E}$  is less than  $10^{-5} W/m^2$  it is set to zero in the Table. Significant changes compared to the baseline (*TE consistent* configuration) discussed in the main text are in bold font.

Descriptor	$N$	$\text{lcp\_moist}$	$f_{\text{type}}$	$\partial \hat{E}_{\text{phys}}^{(p_{\text{work}})}$	$\partial \hat{E}_{\text{phys}}^{(efix)}$	$\partial \hat{E}_{\text{phys}}^{(discr)}$	$\partial \hat{E}_{\text{dyn}}^{(2D)}$	$\partial \hat{E}_{\text{dyn}}^{(heat)}$	$\partial \hat{E}_{\text{dyn}}^{(vis)}$	$\partial \hat{E}_{\text{dyn}}^{(res)}$	$\partial \hat{E}_{\text{dyn}}^{(remap)}$	$\partial \hat{E}_{\text{dyn}}^{(adiab)}$	$\partial \hat{E}_{\text{dyn}}^{(pdc)}$
<i>TE consistent</i>	1	false	1	0.312	0.300	0	-0.601	-0.608	0.565	0.007	-0.011	-0.613	0
‘dribbling’ A	1	false	0	0.315	0.313	0	-0.577	-0.584	0.568	0.007	-0.011	-0.588	<b>0.469</b>
‘dribbling’ B	1	false	2	0.316	0.341	0	-0.598	-0.606	0.563	0.008	-0.011	-0.609	<b>0.484</b>
<i>vert limiter</i>	1	false	1	0.317	0.472	0	-0.590	-0.597	0.509	0.006	<b>-0.199</b>	-0.789	0
<i>smooth topo</i>	1	false	1	0.315	<b>-0.008</b>	0	<b>-0.295</b>	<b>-0.300</b>	0.493	0.005	-0.012	<b>-0.307</b>	0
<i>energy discr</i>	5	true	1	0.332	-0.313	<b>0.594</b>	-0.603	-0.612	0.575	0.009	-0.011	-0.614	-
<i>default</i>	5	true	2	0.316	-0.272	-0.578	-0.587	-0.579	0.579	0.010	-0.012	-0.589	-
<i>QPC6</i>	1	false	1	0.305	-0.169	0	<b>-0.129</b>	<b>-0.131</b>	0.477	0.001	-0.007	<b>-0.136</b>	0
<i>FHS94</i>	1	false	2	-	-	<b>-0.025</b>	<b>-0.025</b>	0.122	0	0.005	<b>-0.020</b>	-	-
<i>FV</i>	1	false	1	0.304	0.670	0	-	-	-	-	<b>-0.974</b>	0	-
<i>CSLAM</i>	1	false	1	0.312	0.239	0	-0.547	-0.557	0.620	0.010	-0.011	-0.558	<b>-0.070</b>
<i>CSLAM default</i>	5	true	2	0.320	-0.342	-	-0.524	-0.537	0.641	0.013	-0.011	-0.535	-

420 32 levels in the vertical. Unless otherwise noted all simulations are 13 months in dura-  
 421 tion and the last 12 months are used in the analysis. Total energy budgets are summarized  
 422 in Table 1 and discussed below. The first column gives identifying ‘Descriptors’ which  
 423 are briefly summarized below and defined in more detail in the following sections. The  
 424 section titles also include the ‘Descriptor’ from Table 1 to make it easier for the reader  
 425 to match Table entries with discussion in the text. Important changes to TE errors are  
 426 marked with bold font in Table 1.

427 Various configurations are used and referred to in terms of the *COMPSET* (Com-  
 428 ponent Set) value used in CESM2.1 The *COMPSET F2000climo* configuration refers  
 429 to ‘real-world’ AMIP (Atmospheric Model Intercomparison Project) type simulations us-  
 430 ing perpetual year 2000 SST (Sea Surface Temperature) boundary conditions. The first 7  
 431 simulations in the table (those above the horizontal line) are such AMIP-type simulations  
 432 (*F2000climo*) with the first serving as a control for the 6 following variants. The remain-  
 433 ing 5 simulation descriptors (below the horizontal line in Table 1) list their *COMPSET* or  
 434 dynamical core settings.

- 435 • *TE consistent*: The TE consistent version uses *state update* physics-dynamics cou-  
 436 pling (*ftype* 1) described in section 3.1,
- 437 • ‘*dribbling*’ A: as *TE consistent* but with *dribbling* physics-dynamics coupling (*ftype*  
 438 0) (section 3.2),
- 439 • ‘*dribbling*’ B: as *TE consistent* but with *dribbling* combination physics-dynamics  
 440 coupling (*ftype* 2) (section 3.2),
- 441 • *vert limiter*: as *TE consistent* but using limiters in the vertical remapping of mo-  
 442 mentum (section 3.3),
- 443 • *smooth topo*: as *TE consistent* but using smoother topography (see section 3.4),
- 444 • *energy discr*: The version with energy discrepancy (but no physics-dynamics cou-  
 445 pling errors) described in section 3.5,
- 446 • *default*: as *energy discr* version but with *ftype*=2 which is the current default  
 447 CAM-SE (section 3.5),
- 448 • *QPC6*: A simplified aqua-planet setup based on the *TE consistent*, i.e an aqua-  
 449 planet setup using CAM6 physics; an ocean covered planet in perpetual equinox,  
 450 with fixed, zonally symmetric sea surface temperatures [Neale and Hoskins, 2000;  
 451 Medeiros et al., 2016] (section 3.6),
- 452 • *FSH94*: Dry dynamical core configuration based on Held-Suarez forcing which re-  
 453 laxes temperature to a zonally symmetric equilibrium temperature profile and sim-  
 454 ple linear drag at the lower boundary [Held and Suarez, 1994] (section 3.7),
- 455 • *FV*: A configuration with the SE dynamical core replaced with the finite-volume  
 456 core (section 3.8), and
- 457 • *CSLAM*: The quasi equal-area physics grid configuration of CAM-SE based on the  
 458 TE consistent setup (section 3.9)
- 459 • *CSLAM default*: Same as *CSLAM* configuration but with *ftype*=2 and all forms of  
 460 water thermodynamically/*inertially* active in the dynamical core.

### 467 3.1 *TE consistent: state-update* physics-dynamics coupling (*ftype*=1) and no TE 468 formula discrepancy

469 This configuration is the most energetically consistent in that the physical parame-  
 470 terizations and the continuous equations of motion on which the dynamical core is based,  
 471 conserve the same TE (defined in equation (8)); and there are no spurious sources/sinks in  
 472 physics-dynamics coupling. Energetic consistency in dynamics and physics is obtained  
 473 by setting  $c_p^{(\ell)} \equiv c_p^d$  and  $\mathcal{L}_{all} = \{\text{`d', 'wv'}\}$  in the dynamical core equations of mo-  
 474 tion and TE computations. Associated namelist changes resulting in this configuration are  
 475 `lcp_moist = .false., se_qsize_condensate_loading = 1, and ftype = 1.`

The TE consistent configuration in AMIP-type simulation (*F2000climo*) is used to compute baseline TE tendencies which will be used to compare with other model configurations. First we establish how long an average is needed to get robust TE tendency estimates. Figure 2 shows  $\partial\widehat{E}$  for various aspects of CAM-SE as a function of time. The simulation length is 5 years and monthly average values are used for the analysis. First consider the left plot. The TE tendency from parameterizations ( $\partial\widehat{E}_{phys}^{(param)}$ ) show significant variability with an amplitude of approximately  $2.5W/m^2$ . As noted above this term does not figure in the spurious TE budget. The net source/sink provides an equal and opposite term to balance it. That said, the variability is reflected onto the TE tendency due to pressure work **error**  $\partial\widehat{E}_{phys}^{(pwork)} \approx 0.32 \pm 0.08W/m^2$ . On the scale used in the left-hand plot the TE tendency of the adiabatic dynamical core  $\partial\widehat{E}_{dyn}^{(adiab)}$  does not seem to be affected by  $\partial\widehat{E}_{phys}^{(param)}$  or  $\partial\widehat{E}_{phys}^{(pwork)}$  in terms of variability, and remains stable at approximately  $-0.6W/m^2 \pm 0.02W/m^2$ . The TE fixer, in this model configuration, fixes  $\partial\widehat{E}_{dyn}^{(adiab)}$  and  $\partial\widehat{E}_{phys}^{(pwork)}$ . Since the TE imbalance in the adiabatic dynamics remains approximately constant and the TE tendency associated with pressure work **error** has variability, the TE tendency from the  $\partial\widehat{E}_{phys}^{(efix)}$  has variability;  $\partial\widehat{E}_{phys}^{(efix)} \approx 0.30 \pm 0.08W/m^2$ . As a consistency check  $-\partial\widehat{E}_{dyn}^{(adiab)} - \partial\widehat{E}_{phys}^{(pwork)}$  is plotted with asterisk's and they coincide (as expected) with  $\partial\widehat{E}_{phys}^{(efix)}$  fulfilling (22).

The right-hand plot in Figure 2 shows a breakdown of the dynamical core TE tendencies. The majority of the TE errors are due to hyperviscosity on temperature and pressure,  $\partial\widehat{E}_{dyn}^{(hvis)} \approx -0.61 \pm 0.01W/m^2$ . The diffusion of momentum is added back as frictional heating and is therefore not part of  $\partial\widehat{E}_{dyn}^{(hvis)}$ . The frictional heating is a significant term in the TE tendency budget  $\partial\widehat{E}_{dyn}^{(fheat)} \approx 0.56 \pm 0.02W/m^2$  and exhibits some variability but with a rather small amplitude. The remaining TE error in the floating Lagrangian dynamics is inviscid dissipation and time-truncation errors  $\partial\widehat{E}_{dyn}^{(res)} = \partial\widehat{E}_{dyn}^{(2D)} - \partial\widehat{E}_{dyn}^{(hvis)} \approx 0.007W/m^2$ . The TE tendency from vertical remapping is approximately  $\partial\widehat{E}_{dyn}^{(remap)} \approx -0.01W/m^2$ . To within  $\sim 0.02W/m^2$  the dynamical core TE tendency terms can be computed from just one month average TE integrals. The TE tendencies computed in physics, excluding  $\partial\widehat{E}_{phys}^{(param)}$ , exhibit more variability and are only accurate to  $\sim 0.1W/m^2$  after a one month average.

While it is advantageous to use *state-update* physics-dynamics coupling algorithm (`fptype=1`) in terms of having no spurious TE tendency from coupling,  $\partial\widehat{E}^{(pdc)} = 0$ , it does result in spurious gravity waves in the simulations [see, e.g., Figure 5 in *Gross et al., 2018*]. Figure 3a shows a 1 year average of  $|\frac{dp_s}{dt}|$ , a measure of high frequency gravity wave noise. It clearly exhibits unphysical oscillations coinciding with element boundaries. Details of the spectral-element method, its coupling to physics and associated noise issues are discussed in detail in *Herrington et al. [2018]*. The noise in the solutions is even visible in the 500hPa pressure velocity annual average (Figure 4a). This issue can be alleviated by using a shorter physics time-step so that the physics increments are smaller (not shown). Climate modelers have historically not pursued a shorter physics time-step in production configurations as climate parameterizations are computationally expensive and there is a large sensitivity to physics time-steps in the simulated climate [e.g. *Williamson and Olson, 2003; Wan et al., 2015*].

### 519 3.2 ‘dribbling’ A/B: Non-TE conservative physics-dynamics coupling (`fptype=0, 2`)

520 Before discussing the impact of different PDC methods on the TE budget, we dis-  
 521 cuss element boundary noise issues in CAM-SE which are related to PDC method. This  
 522 motivates the different PDC methods implemented in CAM-SE.

### 523 3.2.1 Spurious element boundary noise from physics-dynamics coupling

524 When switching to *dribbling* physics-dynamics coupling algorithm (`ftype=0`) in  
 525 which the tendencies from physics are added throughout the dynamics (in this case twice  
 526 per physics time-step) then the noise issues described in previous section disappear (Figure  
 527 3b and 4b). That said, there is a significant issue with this approach; the tracer mass bud-  
 528 getss may not be closed. How this comes about is illustrated in Figure 5 and explained in  
 529 the next paragraph.

530 The orange curve on Figure 5a, b, d, and e is the initial state of, e.g., cloud liq-  
 531 uid mixing ratio as a function of location, e.g., longitude. Cloud liquid is zero outside  
 532 of clouds and hence provides a good example for the purpose of this illustration. The  
 533 light blue arrows show the increments (in terms of length of arrow) computed by the pa-  
 534 rameterizations based on the initial state and scaled for the partial update with *dribbling*  
 535 (`ftype=0`). With *state-update* (`ftype=1`) the increments from physics are added to the  
 536 dynamical core state (dotted line on 5b) before the dynamical core advances the solution  
 537 in time. The parameterizations are designed to not drive the mixing ratios negative so the  
 538 state-update in dynamics will not generate negatives (or overshoots). Then the dynami-  
 539 cal core advects the distribution (solid curve on Figure 5c). With *dribbling* (`ftype=0`) the  
 540 physics increments are split into equal chunks (in this illustration two; blue errors on Fig-  
 541 ure 5d). Half of the physics increments are added to the initial state (dotted line on Fig-  
 542 ure 5e) and then dynamics advects the distribution half of the total dynamical core steps  
 543 (dashed line on Figure 5e). Then the other half of the physics increments are applied (in  
 544 the same location as they were computed by physics). Now after the previous/first advec-  
 545 tion step the cloud liquid distribution has moved and the mixing ratio may be zero (or  
 546 less than the increment prescribed by physics) where the physics forcing is applied (e.g.,  
 547 left side of dashed curve). Hence the physics increment is driving the mixing ratios neg-  
 548 ative in those locations. Thereafter the distribution is advected (solid curve on Figure 5f).  
 549 In CAM the increments added in the dynamical core are limited so that they drive the  
 550 mixing to zero (but not negative) if this problem occurs. This leads to a net source of  
 551 mass compared to the mass change that the parameterizations prescribe (see Figure 6).  
 552 Although the average source of mass is small each time-step it always has the same sign  
 553 (i.e. it is a bias) and therefore accumulates. Zhang *et al.* [2017] estimated that this spuri-  
 554 ous source of mass is equivalent to  $\sim 10\text{cm}$  sea-level rise per decade in coupled climate  
 555 simulation experiments.

556 The majority of the noise with *state-update* (`ftype=1`) physics-dynamics coupling  
 557 method comes from momentum sources/sinks and heating/cooling. A way to alleviate  
 558 noise problems and, at the same time, close the tracer mass budgets (in physics-dynamics  
 559 coupling) is to use *state-update* (`ftype=1`) coupling for tracers and *dribbling* (`ftype=0`)  
 560 coupling for momentum and temperature (referred to as *combination*, `ftype=2`). Figure  
 561 3c shows the noise diagnostic  $|\frac{dp_s}{dt}|$  for *combination* (`ftype=2`) coupling. Figure 3c looks  
 562 very similar to Figure 3b but there is some noise near element boundaries. That said, in  
 563 terms of vertical pressure velocities *combination* (`ftype=2`) and *dribbling* (`ftype=0`) cli-  
 564 mates are similar in terms of the level of noise (Figure 4b and 4c). The element noise in  
 565 CAM-SE with *combination* (`ftype=2`) seen in both  $|\frac{dp_s}{dt}|$  and 500hPa pressure velocity  
 566 can be ‘removed’ by using CAM-SE-CSLAM (Figure 3d) which uses a quasi equal-area  
 567 physics grid and CSLAM [Conservative Semi-LAgrangian Multi-tracer; Lauritzen *et al.*,  
 568 2010] consistently coupled to the SE method [Lauritzen *et al.*, 2017]. The noise patterns  
 569 in vertical velocity off the western coast of South America are present in all CAM-SE  
 570 simulations (and hence not related to physics-dynamics coupling algorithm) are also ‘re-  
 571 moved’ by using CAM-SE-CSLAM [Herrington *et al.*, 2018].

### 572 3.2.2 Spurious TE tendencies from physics-dynamics coupling

573 When using the same TE formula in the dynamical core and physics the spurious  
 574 TE tendency from physics-dynamics coupling can be assessed. As described in item ??  
 575 ([Section 2.2](#)), PDC errors can be attributed to underlying pressure changes during the  
 576 ‘dribbling’ of temperature and velocity component increments as well as PDC ‘clipping’  
 577 errors in the water variables (the process in which ‘clipping’ occurs is described in detail  
 578 in the previous subsection). The TE error associated with ‘clipping’ PDC error occurs due  
 579 to the mass-change prescribed by physics consistent with the fluxes in/out of the physics  
 580 column does not equal the actual mass change applied to the dynamical core state due to  
 581 ‘clipping’

582 For `ftype=2` PDC only the increment for temperature and momentum are *dribbled*  
 583 whereas tracer mass is state-updated (no ‘clipping’ errors). This results in a spurious PDC  
 584 TE tendency of  $\partial\widehat{E}^{(pdc)} = -0.484W/m^2$ . When using `ftype=0` PDC also tracer increments  
 585 are *dribbled* (hence there are ‘clipping’ PDC errors) a similar TE tendency results  
 586  $\partial\widehat{E}^{(pdc)} = -0.469W/m^2$ . The difference between the TE PDC tenendency for `ftype=2`  
 587 and `ftype=0` provides an estimate of the TE PDC ‘clipping’ error. The ‘clipping’ PDC  
 588 TE tenendency is very small  $0.015W/m^2$ .

### 589 3.3 *vert limiter*: Limiters on vertical remapping of momentum

590 CAM-SE uses a floating Lagrangian vertical coordinate [[Starr, 1945](#); [Lin, 2004](#)]  
 591 which requires the remapping of the atmospheric state from floating levels back to refer-  
 592 ence levels to maintain computational stability and to provide state data consistent with  
 593 the physics formulation. The mapping algorithm is based on the mass conservative PPM  
 594 (Piecewise Parabolic Method) with options for shape-preserving limiters. In CAM-SE mo-  
 595 mentum components and internal energy are used as the variables mapped in the vertical  
 596 [[Lauritzen et al., 2018](#)] and, contrary to earlier versions of CAM-SE, there is no limiter  
 597 on the remapping of wind components. If the shape-preserving limiter is used for mo-  
 598 mentum mapping then the TE dissipation increases by over an order of magnitude from  
 599  $\sim 0.01W/m^2$  to  $\sim 0.2W/m^2$  (Table 1).

### 600 3.4 *smooth topo*: Smoother topography

601 Topography for CAM is generated using a new version of the software/algorithm de-  
 602 scribed in [Lauritzen et al. \[2015\]](#) that is available at <https://github.com/NCAR/Topo>.  
 603 The updates to the software includes smoothing algorithms and the computation of sub-  
 604 grid-scale orientation of topography.

605 The default topography in CAM-SE uses the same amount of topography smooth-  
 606 ing as CAM-FV (distance weighted smoother applied to the raw topography on  $\sim 3\text{km}$   
 607 cubed-sphere grid with a smoothing radius of 180km referred to as C60). When the to-  
 608 polography is smoother (in this case using C92 smoothing, i.e. smoothing radius of approx-  
 609 imately 276km) the hyperviscosity operators are less active leading to reduced TE errors,  
 610 i.e.  $\partial\widehat{E}_{dyn}^{(hv)}$  is reduced in half from approximately  $-0.6W/m^2$  to  $-0.3W/m^2$ . The vertical  
 611 remapping TE error, however, remains approximately the same. Since the pressure work  
 612 [error](#) is approximately  $0.3W/m^2$  it almost exactly compensates for the TE tendency from  
 613 the dynamical core  $\partial\widehat{E}_{dyn}^{(adiab)}$ . Hence if one would only diagnose the TE tendency from  
 614 the energy fixer one could mistakenly conclude that the model universally conserves TE  
 615 when, in fact, there are compensating TE errors in the system. These compensating errors  
 616 can only be diagnosed through a careful breakdown of the total TE tendencies.

### 617 3.5 default: TE formula discrepancy errors

618 To assess the TE errors due to the discrepancy in the energy formula used by dy-  
 619 namics and physics, a simulation using *state-updating* (`ftype=1`, no ‘*dribbling* errors) and  
 620 thermodynamically/*inertially* active condensates in the dynamical core (`qsize_condensate_loading =`  
 621  $5$ ) and consistent/accurate associated heat capacities  $c_p^{(\ell)}$  (namelist `1cp_moist=.true.`)  
 622 has been performed. In this setup the continuous equations of motion in the dynami-  
 623 cal core conserve an energy different from physics, and the energy fixer will restore the  
 624 ‘physics’ version of energy. Despite the dynamical core now using a more comprehensive  
 625 formula for energy, the TE dissipation terms in the dynamical core are roughly the same  
 626 as in the energy consistent versions of the model. Using (25) we can assess the TE energy  
 627 discrepancy errors which result in  $\sim 0.59W/m^2$ . *Taylor* [2011] found a similar result just  
 628 from using the more comprehensive formula for heat capacity (based on dry air and water  
 629 vapor) and not including thermodynamically/*inertially* active condensates. As noted before  
 630 this formulation inconsistency is due to the evolutionary nature of CAM development and  
 631 it is the intention to remove this inconsistency in future versions of the model.

632 The default version of CAM-SE uses this configuration but with *combination* (`ftype=2`)  
 633 which has similar TE characteristics (see Table 1). That said, the physics-dynamics cou-  
 634 pling error from *dribbling* momentum and temperature tendencies and the energy discrep-  
 635 ancny errors can not be separated in this configuration:

$$\partial \widehat{E}^{(pdc)} + \partial \widehat{E}^{(discr)} = 0.546W/m^2, \quad (27)$$

636 using (22). With *state-updating* (`ftype=1`) (i.e.  $\partial \widehat{E}^{(pdc)} = 0$ ) the energy discrepancy error  
 637 was  $0.594W/m^2$  and in the energy consistent setup (i.e.  $\partial \widehat{E}^{(discr)} = 0$ ) but using *dribbling*  
 638 (`ftype=2`) we got  $\partial \widehat{E}^{(pdc)} = 0.484W/m^2$ . So if the physics-dynamics coupling errors  
 639 and energy discrepancy errors in the different configurations would be additive, one would  
 640 have expected  $\partial \widehat{E}^{(pdc)} + \partial \widehat{E}^{(discr)}$  to be over  $1W/m^2$  which is clearly not the case (26).  
 641 Again, it must be concluded that there are canceling errors in the system.

### 642 3.6 QPC6: Simplified surface

643 By running the model in aqua-planet configuration one can assess the effect of sim-  
 644 plifying the surface boundary condition. In particular, without topography forcing the dy-  
 645 namical core is not challenged with respect to stationary near-grid-scale forcing. The TE  
 646 tendency with respect to pressure work *error* remains the same  $\partial \widehat{E}_{phys}^{(pwork)}$  as the AMIP-  
 647 type simulations, however, the adiabatic dynamical core TE tendency reduces to  $\partial \widehat{E}_{dyn}^{(adiab)} =$   
 648  $-0.14W/m^2$  (approximately a factor 4 reduction). Most of that reduction is due to viscos-  
 649 ity  $\partial \widehat{E}_{dyn}^{(hvis)} = -0.13W/m^2$ . The frictional heating is roughly the same as AMIP  $\partial \widehat{E}_{dyn}^{(fheat)} =$   
 650  $0.48W/m^2$  as is the vertical remapping  $\partial \widehat{E}_{dyn}^{(remap)} = -0.01W/m^2$ . To evaluate the dynam-  
 651 ical cores diffusion of TE it is therefore important to asses the model in a configuration  
 652 with topography as the wave dynamics generated by topography leads to more active dif-  
 653 fusion operators.

### 654 3.7 FHS94: Simplified physics (no moisture)

655 Simplifying the setup even further by replacing the parameterizations with relax-  
 656 ation towards a zonally symmetric temperature profile and simple boundary layer friction  
 657 (Held-Suarez forcing) as well as excluding moisture, the TE errors in the dynamical core  
 658 decreases even further to  $\sim 0.002W/m^2$  since there is no small scale forcing. Small scales  
 659 are only created by the nonlinear dynamics and the physics works to damp them. Hyper-  
 660 viscosity is less active leading to significant reductions compared to aqua-planet and ‘real-  
 661 world’ simulation results. The TE diffusion in vertical remapping reduces by an order of  
 662 magnitude compared to the aqua-planet simulations ( $\sim 0.0005W/m^2$ ). This further em-  
 663 phasizes that TE diffusion assessment in a simplified setup is not necessarily telling for

664 the dynamical cores performance with moist physics and topography that challenge the  
 665 dynamical core in terms of strong grid-scale forcing.

### 666 3.8 FV: Changing dynamical core to Finite-Volume (FV)

667 As a comparison the TE error characteristics of the CAM-FV dynamical core are  
 668 assessed. Although the TE diagnostics have not been implemented in the CAM-FV dy-  
 669 namical core, the TE diagnostics in CAM physics are independent of dynamical core  
 670 and can therefore be activated with CAM-FV. The CAM-FV dynamical core uses *state-*  
 671 *update* physics-dynamics coupling (`fptype=1`) ( $\partial\widehat{E}^{(pdc)} = 0$ ) and the same TE definition  
 672 as CAM physics ( $\partial\widehat{E}^{(discr)} = 0$ ). Hence (23) can be used to compute the TE errors of  
 673 the CAM-FV dynamical core,  $\partial\widehat{E}_{dyn}^{(adiab)} \approx -1W/m^2$ . As we do not have the break-down  
 674 of  $\partial\widehat{E}_{dyn}^{(adiab)}$  it can not be determined how much of the TE errors are due to the vertical  
 675 remapping. Furthermore, CAM-FV contains intrinsic dissipation operators (limiters in the  
 676 flux operators) making it difficult to assess TE sources/sinks due to dissipation. Note that  
 677 the pressure work **error** even with a change of dynamical core remains approximately the  
 678 same as the CAM-SE configurations.

### 679 3.9 CSLAM: Quasi equal-area physics grid

680 This configuration was discussed in the context of element noise in section 3.2.1.  
 681 By averaging the dynamics state of an equal-partitioning (in central angle cubed-sphere  
 682 coordinates) of the elements, the element-boundary noise found in CAM-SE can be re-  
 683 moved. Lauritzen *et al.* [2018] argue that this way of computing the state for the physics  
 684 is more consistent with physics in terms of providing a cell-averaged state instead of ir-  
 685 regularly spaced point (quadrature) values. In order to achieve a closed mass-budget, this  
 686 configuration uses CSLAM for tracer transport rather than SE transport. That said, the  
 687 physics columns no longer coincide with the quadrature grid and there are TE errors asso-  
 688 ciated with mapping state and tendencies between the two grids.

689 In this configuration the energy diagnostics computed in the dynamical core are  
 690 computed on the quadrature grid and the energy diagnostics computed in physics are on  
 691 the physics grid. If the TE consistent configuration is used (`fptype=1, qsize_condensate_loading=1,`  
 692 `lcp_moist=.false.`) then the physics-dynamical coupling errors,  $\widehat{E}^{(pdc)}$  computed with  
 693 (20), are entirely due to mapping state from quadrature grid to physics grid and map-  
 694 ping tendencies back the quadrature grid from the physics grid. The results is  $\widehat{E}^{(pdc)} =$   
 695  $-0.07W/m^2$  which is a rather small error compared to other terms in the TE budget.

696 Due to similar noise problems with CAM-SE-CSLAM when using `fptype=1` that  
 697 were observed in CAM-SE (Figure 3 and 4), the default version of CAM-SE-CSLAM uses  
 698 `fptype=2`. Again physics-dynamics coupling errors and TE discrepancy errors can not be  
 699 separated;  $\partial\widehat{E}^{(pdc)} + \partial\widehat{E}^{(discr)} = 0.557W/m^2$ .

## 702 4 Conclusions

703 A detailed total energy (TE) error analysis of the Community Atmosphere Model  
 704 (CAM) using version 6 physics (included in the CESM2.1 release) running at approxi-  
 705 mately 1° horizontal resolution has been presented. In the global climate model there can  
 706 be many spurious contributions to the TE budget. These errors can be divided into four  
 707 categories: physical parameterizations, adiabatic dynamical core, the coupling between  
 708 physics and dynamics, and TE definition discrepancies between dynamics and physics.  
 709 The latter is not by design but through the evolutionary nature of model development. By  
 710 capturing the atmospheric state at various locations in the model algorithm, a detailed  
 711 budget of TE errors can be constructed. The net spurious TE energy errors are compen-

712 sated with a global energy fixer (providing a global uniform temperature increment) every  
 713 physics time-step.

714 In CAM physics the parameterizations have, by design, a closed energy budget (change  
 715 in TE is balanced by fluxes in/out the top and bottom of physics columns) if it is assumed  
 716 that pressure is not modified. However, the pressure changes due to fluxes of mass (e.g.,  
 717 water vapor) in/out of the column which changes energy (referred to as pressure work  
 718 **error**). The pressure work **error** with the full moist physics configuration is very stable  
 719 across different configurations at  $\sim 0.3W/m^2$ . The TE errors in the spectral element (SE)  
 720 dynamical core varies across configurations. Aspects that influence TE is the presence  
 721 of topography, the amount of topography smoothing and moist physics. By smoothing  
 722 topography more the TE error is cut in half from  $\sim -0.6W/m^2$  to  $\sim -0.3W/m^2$ ; and re-  
 723 duces by a factor of **six** ( $\sim -0.1W/m^2$ ) if no topography is present at all (aqua-planet  
 724 configuration). Moist physics forcing also contributes significantly to the TE budget. For  
 725 example, in the dry Held-Suarez setup TE dissipation of the SE dynamical core reduces  
 726 to  $-0.03W/m^2$ . Topography and moist physics force the dynamical core at the grid scale  
 727 and hence the viscosity operators are more active. Consistent with this statement is that  
 728 the changes in TE discussed so far are almost entirely due to the viscosity operator TE  
 729 dissipation. For CAM-SE the spurious TE dissipation in the adiabatic dynamical core is  
 730  $\sim -0.6W/m^2$  in ‘real-world’ configurations. For comparison, CAM-FV’s spurious TE  
 731 change due to the adiabatic dynamical core is  $\sim -1W/m^2$ .

732 By further breaking down the TE dissipation in the SE dynamical core it is ob-  
 733 served the vertical remapping accounts for only  $\sim -0.01W/m^2$ . That said, if the shape-  
 734 preserving limiters in the vertical remapping are invoked the TE dissipation increases 20-  
 735 fold to  $\sim -0.2W/m^2$ . In CAM-SE the kinetic energy dissipation is added as heating in  
 736 the thermodynamic equation (also referred to as frictional heating). The frictional heat-  
 737 ing remains very stable across configurations that include moisture ( $\sim 0.5W/m^2$ ) and re-  
 738 duces drastically for dry atmosphere setups (factor 4 reduction to ( $\sim 0.12W/m^2$ )). Hence  
 739 this term is an important term in the TE budget. The TE budget for the dynamical core  
 740 is dominated by TE change due to hyperviscosity; TE errors due to time-truncation and  
 741 frictionless equations of motion are negligible. Errors associated with physics-dynamics  
 742 coupling (if applicable) are approximately  $0.5W/m^2$ . Due to the evolutionary nature of  
 743 model development the SE dynamical core’s continuous equation of motion conserve a  
 744 more comprehensive TE compared to the physical parameterizations. This TE discrep-  
 745 acy leads to an approximately  $0.5W/m^2$  total energy source. Running physics on a dif-  
 746 ferent grid than the dynamical introduces TE mapping errors such as in CAM-SE-CSLAM  
 747 (Conservative Semi-Lagrangian Multi-tracer transport scheme). These errors are, however,  
 748 rather small  $-0.07W/m^2$ .

749 A purpose of this paper is to better understand the energy characteristics of CAM  
 750 and to encourage modeling groups to perform similar analysis to better understand the  
 751 total energy flow in the atmospheric component of Earth system models. As has been  
 752 demonstrated in this paper there can easily be compensating errors in the system which  
 753 can not be identified without a detailed TE analysis.

#### 754 Acknowledgments

755 The National Center for Atmospheric Research is sponsored by the National Science Foun-  
 756 dation. Computing resources ([doi:10.5065/D6RX99HX](https://doi.org/10.5065/D6RX99HX)) were provided by the Climate  
 757 Simulation Laboratory at NCAR’s Computational and Information Systems Laboratory,  
 758 sponsored by the National Science Foundation and other agencies. The data used to per-  
 759 form the energy analysis can be found at <https://github.com/PeterHjortLauritzen/2018-JAMES-energy>.

761 **References**

- 762 Boville, B. (2000), chap. Toward a complete model of the climate system in Numerical  
 763 Modeling of the Global Atmosphere in the Climate System, pp. 419–442, Springer  
 764 Netherlands.
- 765 Computational and Information Systems Laboratory (2017), Cheyenne: HPE/SGI ICE XA  
 766 System (Climate Simulation Laboratory), Boulder, CO: National Center for Atmospheric  
 767 Research, doi:10.5065/D6RX99HX.
- 768 Eldred, C., and D. Randall (2017), Total energy and potential enstrophy conserv-  
 769 ing schemes for the shallow water equations using hamiltonian methods – part  
 770 1: Derivation and properties, *Geosci. Model Dev.*, 10(2), 791–810, doi:10.5194/  
 771 gmd-10-791-2017.
- 772 Gross, M., H. Wan, P. J. Rasch, P. M. Caldwell, D. L. Williamson, D. Klocke,  
 773 C. Jablonowski, D. R. Thatcher, N. Wood, M. Cullen, B. Beare, M. Willett, F. Lemarié,  
 774 E. Blayo, S. Malardel, P. Termonia, A. Gassmann, P. H. Lauritzen, H. Johansen, C. M.  
 775 Zarzycki, K. Sakaguchi, and R. Leung (2018), Physics-dynamics coupling in weather,  
 776 climate and earth system models: Challenges and recent progress, *Mon. Wea. Rev.*, 146,  
 777 3505–3544, doi:10.1175/MWR-D-17-0345.1.
- 778 Held, I. M., and M. J. Suarez (1994), A proposal for the intercomparison of the dynamical  
 779 cores of atmospheric general circulation models, *Bull. Amer. Meteor. Soc.*, 75, 1825–  
 780 1830.
- 781 Herrington, A. R., P. H. Lauritzen, M. A. Taylor, S. Goldhaber, B. E. Eaton, K. A. Reed,  
 782 and P. A. Ullrich (2018), Physics-dynamics coupling with element-based high-order  
 783 Galerkin methods: quasi equal-area physics grid, *Mon. Wea. Rev.*
- 784 Jablonowski, C., and D. L. Williamson (2011), chap. The Pros and Cons of Diffusion,  
 785 Filters and Fixers in Atmospheric General Circulation Models, pp. 381–493, Springer  
 786 Berlin Heidelberg, Berlin, Heidelberg, doi:10.1007/978-3-642-11640-7\_13.
- 787 Kasahara, A. (1974), Various vertical coordinate systems used for numerical weather pre-  
 788 diction, *Mon. Wea. Rev.*, 102(7), 509–522.
- 789 Lauritzen, P. H., R. D. Nair, and P. A. Ullrich (2010), A conservative semi-Lagrangian  
 790 multi-tracer transport scheme (CSLAM) on the cubed-sphere grid, *J. Comput. Phys.*,  
 791 229, 1401–1424, doi:10.1016/j.jcp.2009.10.036.
- 792 Lauritzen, P. H., J. T. Bacmeister, T. Dubos, S. Lebonnois, and M. A. Taylor (2014),  
 793 Held-Suarez simulations with the Community Atmosphere Model Spectral Element  
 794 (CAM-SE) dynamical core: A global axial angular momentum analysis using Eule-  
 795 rian and floating Lagrangian vertical coordinates, *J. Adv. Model. Earth Syst.*, 6, doi:  
 796 10.1002/2013MS000268.
- 797 Lauritzen, P. H., J. T. Bacmeister, P. F. Callaghan, and M. A. Taylor (2015), NCAR\_Topo  
 798 (v1.0): NCAR global model topography generation software for unstructured grids,  
 799 *Geosci. Model Dev.*, 8(12), 3975–3986, doi:10.5194/gmd-8-3975-2015.
- 800 Lauritzen, P. H., M. A. Taylor, J. Overfelt, P. A. Ullrich, R. D. Nair, S. Goldhaber, and  
 801 R. Kelly (2017), CAM-SE-CSLAM: Consistent coupling of a conservative semi-  
 802 lagrangian finite-volume method with spectral element dynamics, *Mon. Wea. Rev.*,  
 803 145(3), 833–855, doi:10.1175/MWR-D-16-0258.1.
- 804 Lauritzen, P. H., R. Nair, A. Herrington, P. Callaghan, S. Goldhaber, J. Dennis, J. T.  
 805 Bacmeister, B. Eaton, C. Zarzycki, M. A. Taylor, A. Gettelman, R. Neale, B. Dobbins,  
 806 K. Reed, and T. Dubos (2018), NCAR release of CAM-SE in CESM2.0: A reformu-  
 807 lation of the spectral-element dynamical core in dry-mass vertical coordinates with  
 808 comprehensive treatment of condensates and energy, *J. Adv. Model. Earth Syst.*, doi:  
 809 10.1029/2017MS001257.
- 810 Lin, S.-J. (2004), A 'vertically Lagrangian' finite-volume dynamical core for global mod-  
 811 els, *Mon. Wea. Rev.*, 132, 2293–2307.
- 812 McRae, A. T. T., and C. J. Cotter (2013), Energy- and enstrophy-conserving schemes for  
 813 the shallow-water equations, based on mimetic finite elements, *Quart. J. Roy. Meteor.  
 814 Soc.*, 140(684), 2223–2234, doi:10.1002/qj.2291.

- 815 Medeiros, B., D. L. Williamson, and J. G. Olson (2016), Reference aquaplanet climate in  
 816 the community atmosphere model, version 5, *J. Adv. Model. Earth Syst.*, 8(1), 406–424,  
 817 doi:10.1002/2015MS000593.
- 818 Neale, R. B., and B. J. Hoskins (2000), A standard test for AGCMs including their phys-  
 819 ical parametrizations: I: the proposal, *Atmos. Sci. Lett.*, 1(2), 101–107, doi:10.1006/asle.  
 820 2000.0022.
- 821 Neale, R. B., C.-C. Chen, A. Gettelman, P. H. Lauritzen, S. Park, D. L. Williamson, A. J.  
 822 Conley, R. Garcia, D. Kinnison, J.-F. Lamarque, D. Marsh, M. Mills, A. K. Smith,  
 823 S. Tilmes, F. Vitt, P. Cameron-Smith, W. D. Collins, M. J. Iacono, R. C. Easter, S. J.  
 824 Ghan, X. Liu, P. J. Rasch, and M. A. Taylor (2012), Description of the NCAR Commu-  
 825 nity Atmosphere Model (CAM 5.0), *NCAR Technical Note NCAR/TN-486+STR*, National  
 826 Center of Atmospheric Research.
- 827 Skamarock, W. C., J. B. Klemp, M. G. Duda, L. Fowler, S.-H. Park, and T. D. Ringler  
 828 (2012), A multi-scale nonhydrostatic atmospheric model using centroidal Voronoi tes-  
 829 selations and C-grid staggering, *Mon. Wea. Rev.*, 140, 3090–3105, doi:doi:10.1175/  
 830 MWR-D-11-00215.1.
- 831 Starr, V. P. (1945), A quasi-Lagrangian system of hydrodynamical equations., *J. Atmos.*  
 832 *Sci.*, 2, 227–237.
- 833 Taylor, M. A. (2011), Conservation of mass and energy for the moist atmospheric prim-  
 834 itive equations on unstructured grids, in: P.H. Lauritzen, R.D. Nair, C. Jablonowski,  
 835 M. Taylor (Eds.), Numerical techniques for global atmospheric models, *Lecture Notes*  
 836 *in Computational Science and Engineering*, Springer, 2010, *in press.*, 80, 357–380, doi:  
 837 10.1007/978-3-642-11640-7\_12.
- 838 Thuburn, J. (2008), Some conservation issues for the dynamical cores of NWP and cli-  
 839 mate models, *J. Comput. Phys.*, 227, 3715–3730.
- 840 Trenberth, K. E., and J. T. Fasullo (2018), Applications of an updated atmospheric ener-  
 841 getics formulation, *J. Climate*, 31(16), 6263–6279, doi:10.1175/JCLI-D-17-0838.1.
- 842 Wan, H., P. J. Rasch, M. A. Taylor, and C. Jablonowski (2015), Short-term time step con-  
 843 vergence in a climate model, *J. Adv. Model. Earth Syst.*, 7(1), 215–225, doi:10.1002/  
 844 2014MS000368.
- 845 Williamson, D. L. (2002), Time-split versus process-split coupling of parameterizations  
 846 and dynamical core, *Mon. Wea. Rev.*, 130, 2024–2041.
- 847 Williamson, D. L., and J. G. Olson (2003), Dependence of aqua-planet simulations on  
 848 time step, *Q. J. R. Meteorol. Soc.*, 129(591), 2049–2064.
- 849 Williamson, D. L., J. G. Olson, C. Hannay, T. Toniazzo, M. Taylor, and V. Yudin (2015),  
 850 Energy considerations in the community atmosphere model (cam), *J. Adv. Model. Earth*  
 851 *Syst.*, 7(3), 1178–1188, doi:10.1002/2015MS000448.
- 852 Zhang, K., P. J. Rasch, M. A. Taylor, H. Wan, L.-Y. R. Leung, P.-L. Ma, J.-C. Golaz,  
 853 J. Wolfe, W. Lin, B. Singh, S. Burrows, J.-H. Yoon, H. Wang, Y. Qian, Q. Tang,  
 854 P. Caldwell, and S. Xie (2017), Impact of numerical choices on water conservation in  
 855 the e3sm atmosphere model version 1 (eam v1), *Geoscientific Model Development Dis-  
 856 cussions*, 2017, 1–26, doi:10.5194/gmd-2017-293.

```

do nt=1,ntotal

PARAMETERIZATIONS:
Last dynamics state received from dynamics
output 'pBF'
efix Energy fixer
output 'pBP'
phys param Physics updates the state and state saved for energy fixer
output 'pAP'
pwork Pressure work (dry mass correction)
output 'pAM'
Physics tendency (forcing) passed to dynamics

DYNAMICAL CORE
output 'dED'
do ns=1,nsplit
output 'dAF'

phys
START PHYSICS-DYNAMICS COUPLING
Update dynamics state with (1/nsplit) of physics tendency (ftype=2)
if (ns=1) Update dynamics state with entire physics tendency (ftype=1)
DONE PHYSICS-DYNAMICS COUPLING

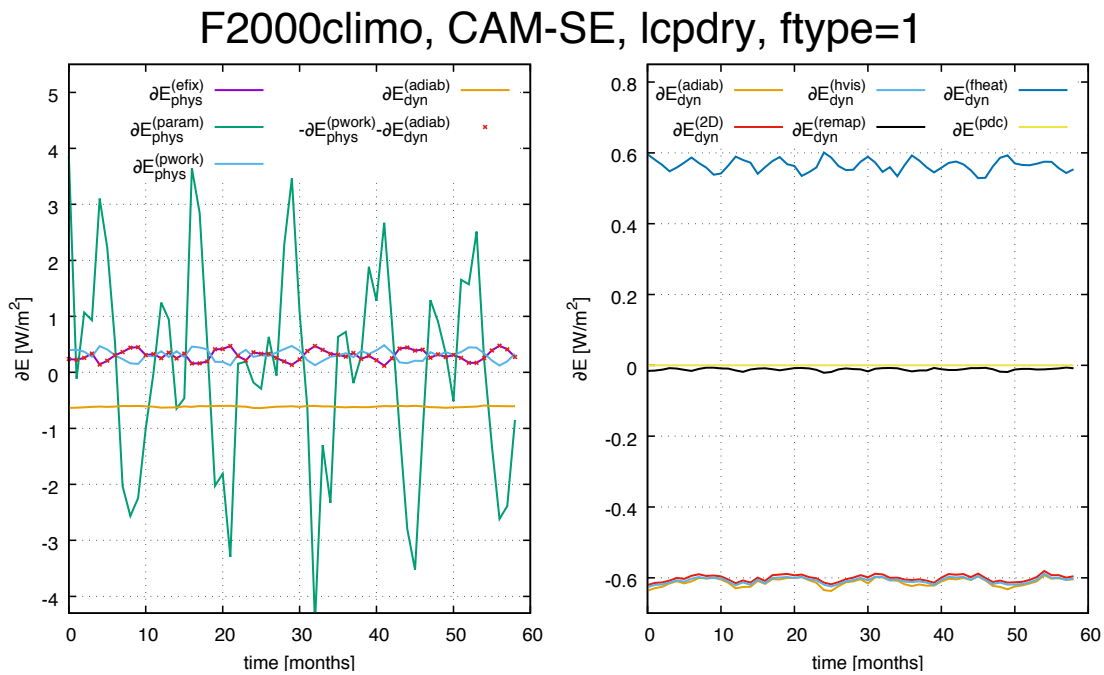
output 'dB'D'

adiab
2D
hvis
do nr=1,rsplit
Advance the adiabatic frictionless equations of motion
in floating Lagrangian layer
do ns=1,hypervis_subcycle
output 'dBH'
Apply hyperviscosity operators
output 'dCH'
fheat Add frictional heating to temperature
output 'dAH'
end do (ns=1,hypervis_subcycle)
end do (nr=1,rsplit)
output 'dAD'
remap
Vertical remapping from floating Lagrangian levels to Eulerian levels
output 'dAR'
end do (ns=1,nsplit)
Dynamics state saved for next model time step and passed to physics
output 'dB'F'

end do (nt=1,ntotal)

```

312 **Figure 1.** Pseudo-code for CAM-SE showing the order in which relevant physics updates are performed as  
 313 well as dynamical core steps and associated loops. In green font locations where the state is captured and out-  
 314 put is shown together with its 3 character identifier. The outer most loop (1, *ntotal*) advances the entire model  
 315  $\Delta t_{phys}$  seconds (in this case 1800s). The dynamical core loops are as follows: the outer loop is the vertical  
 316 remapping loop (1, *nsplit*) with associated time-step  $\Delta t_{phys}/nsplit$ . For stability the temporal advance-  
 317 ment of the equations of motion in the Lagrangian layer needs to be sub-cycled *rsplit* times. Within the  
 318 *rsplit*-loop the hyperviscosity time-stepping is sub-cycled *hypervis\_subcycle* times (again for stability).  
 319 For more details on the time-stepping in CAM-SE see Lauritzen *et al.* [2018].



461 **Figure 2.** Monthly averaged TE tendencies as a function of time for various aspects of the TE consistent  
 462 configuration of CAM-SE run in AMIP-type configuration with perpetual year 2000 SSTs. Left Figure shows  
 463  $\partial \hat{E}$  TE tendencies in physics and, for comparison, TE tendency for the adiabatic dynamical core. The right  
 464 plot shows the break-down of  $\partial \hat{E}$  for the dynamical core. These plots show that the energy tendency from the  
 465 dynamical core is quite constant (to within  $\sim 0.02 W/m^2$  or less) so only one month simulations is adequate to  
 466 assess energy diagnostics for the dynamical core. For more details see Section 3.1.

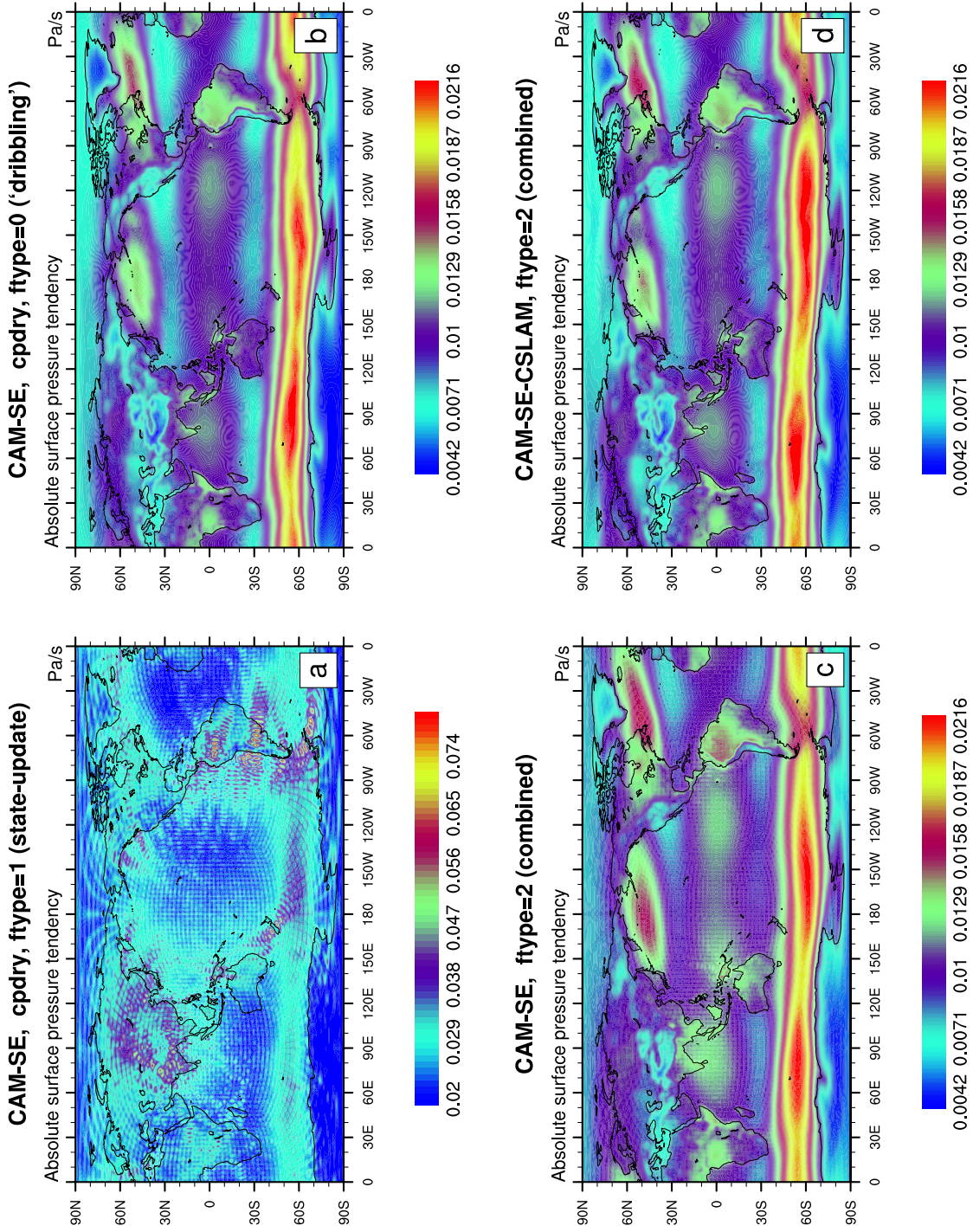


**Figure 3.** One year average of the absolute surface pressure tendency for (a) the TE consistent configuration, (b) ‘dribbling’ physics-dynamics coupling, (c) ftype=2 physics-dynamics coupling and (d) CSLAM version of CAM-SE, respectively. (a) has a closed physics-dynamics coupling budget but spurious noise, (b) has no spurious noise but the mass-budget in physics-dynamics coupling is not closed (see Figure 6), (c) has a closed mass budget in physics-dynamics coupling but some spurious noise at element boundaries which is eliminated when using CAM-SE-CSLAM (d). Note, the smallest value in panel (a) is the largest in panels (b), (c) and (d).

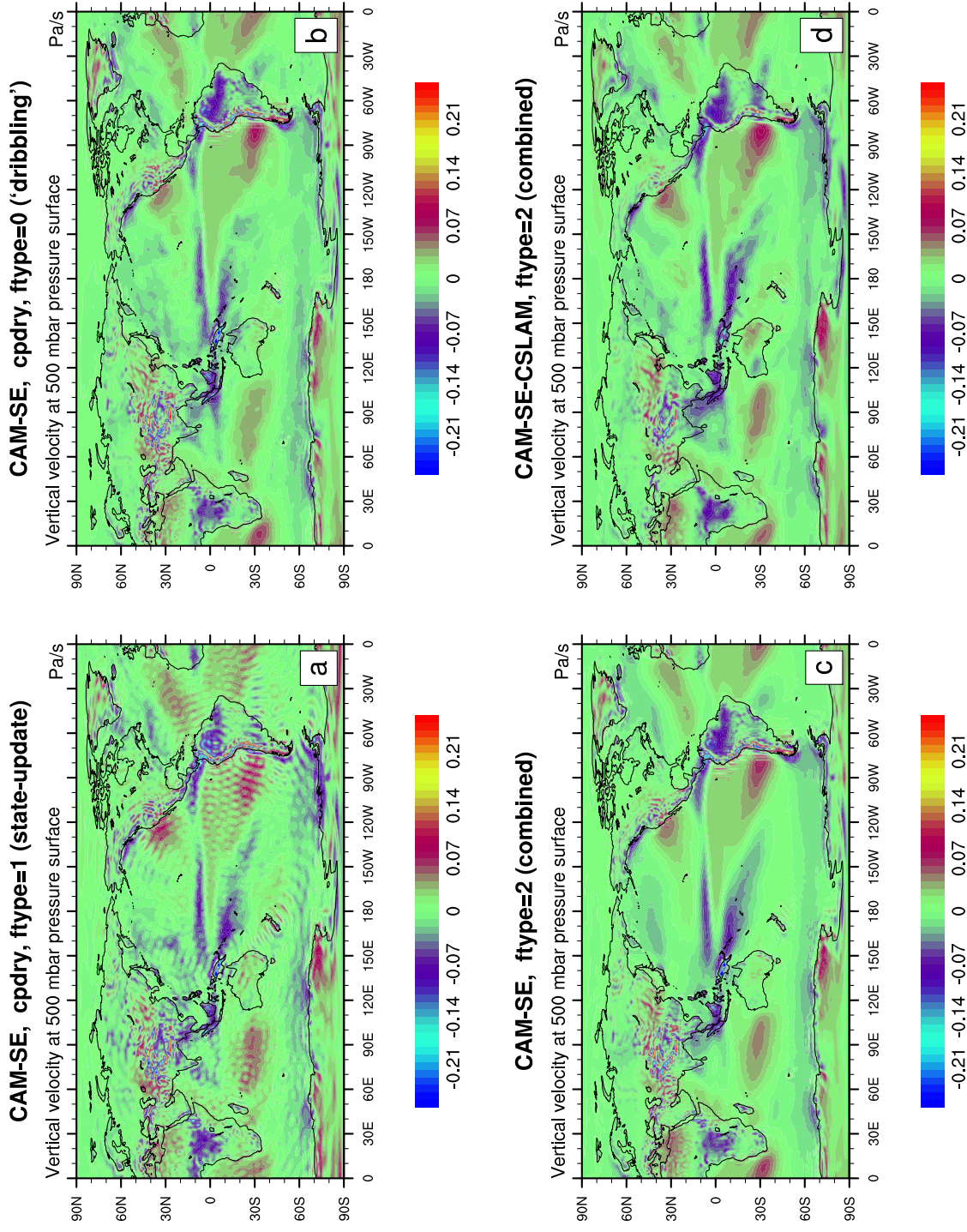


**Figure 4.** Same as Figure 3 but for 500hPa vertical pressure velocity. Note the ringing patterns off the West coast of South America and around the Himalayas in CAM-SE (a-c) that are eliminated with CAM-SE-CSLAM (d) that makes use of a quasi equal-area physics grid.

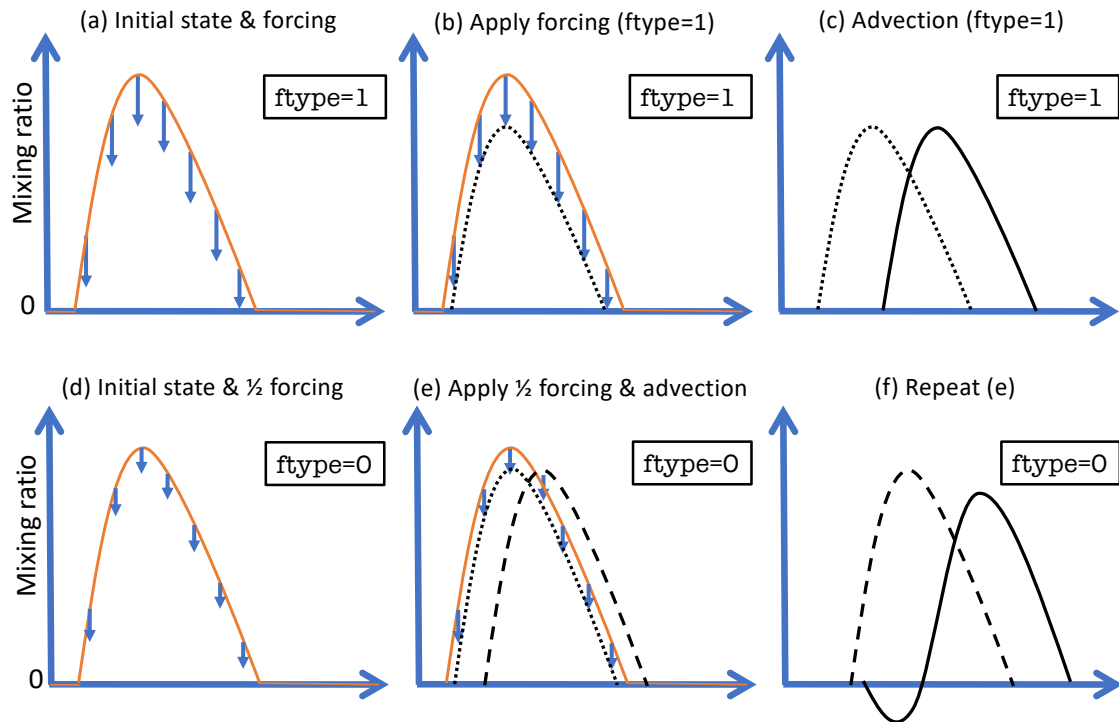


**Figure 5.** A schematic of state-update ( $\text{ftype}=1$ ; row 1) and ‘dribbling’ ( $\text{ftype}=0$ ; row 2) physics-dynamics coupling algorithms. See Section 3.2 for details.

## F2000climo, CAM-SE, cpdry, ftype=0 ('dribbling')

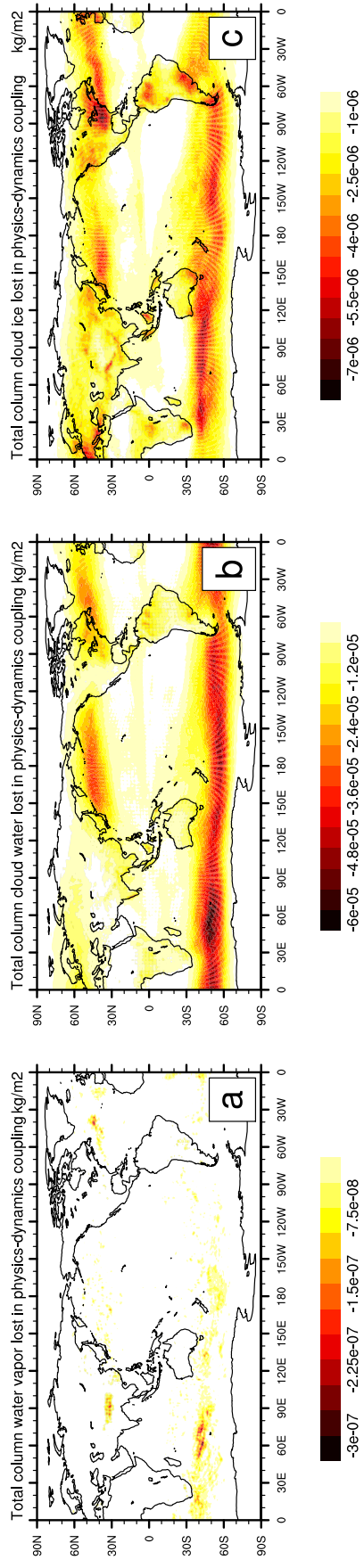


**Figure 6.** One year average of mass  $[kg/m^2]$  'clipped' in physics-dynamics coupling (so that state is not driven negative) when using `ftype=0` ('dribbling') physics-dynamics coupling for (a) water vapor, (b) cloud liquid and (c) cloud ice, respectively. Interestingly the element boundaries systematically show in the plots which is likely related to the anisotropy of the quadrature grid [Herrington *et al.*, 2018].